Exp Brain Res (2013) 224:591–603
DOI 10.1007/s00221-012-3335-x

RESEARCH ARTICLE

The leading joint hypothesis for spatial reaching arm motions

Satyajit Ambike · James P. Schmiedeler

Received: 29 May 2012 / Accepted: 1 November 2012 / Published online: 11 December 2012

Abstract The leading joint hypothesis (LJH), developed for planar arm reaching, proposes that the interaction torques experienced by the proximal joint are low compared to the corresponding muscle torques. The human central nervous system could potentially ignore these interaction torques at the proximal (*leading*) joint with little effect on the wrist trajectory, simplifying joint-level control. This paper investigates the extension of the LJH to spatial reaching. In spatial motion, a number of terms in the governing equation (Euler's angular momentum balance) that vanish for planar movements are non-trivial, so their contributions to the joint torque must be classified as net, interaction or muscle torque. This paper applies definitions from the literature to these torque components to establish a general classification for all terms in Euler's equation. This classification is equally applicable to planar and spatial motion. Additionally, a rationale for excluding gravity torques from the torque analysis is provided. Subjects performed point-to-point reaching movements between targets whose locations ensured that the wrist paths lay in various portions of the arm's spatial workspace. Movement kinematics were recorded using electromagnetic sensors located on the subject's arm segments and thorax. The arm was modeled as a three-link kinematic chain with idealized spherical and revolute joints at the shoulder and elbow. Joint torque components were computed using inverse dynamics. Most movements were 'shoulder-led' in that the interaction torque impulse was significantly lower than the muscle torque impulse for the shoulder, but not the elbow. For the few elbow-led movements, the interaction impulse at the elbow was low, while that at the shoulder was high, and these typically involved large elbow and small shoulder displacements. These results support the LJH and extend it to spatial reaching motion.

Keywords Spatial arm reaching · Leading joint hypothesis · Joint torque partitioning

S. Ambike (✉)
Department of Kinesiology, The Pennsylvania State University, University Park, PA, USA
e-mail: ssa17@psu.edu

J. P. Schmiedeler
Department of Aerospace and Mechanical Engineering, University of Notre Dame, Notre Dame, IN, USA
e-mail: schmiedeler.4@nd.edu

Introduction

In multi-joint serial chains, torque application at one joint instantaneously creates motion at all joints of the chain. This phenomenon is called 'dynamic coupling' (Zajac and Gordon 1989). Consequently, to produce a desired hand trajectory with the human arm, which is often modeled as a multi-joint serial chain, the torque at any joint must be composed by taking into account the movement of *all* joints. How the descending neural commands that produce joint torques are adjusted to these passive, internal *interaction torques or effects* that underlie dynamic coupling has intrigued researchers as early as Bernstein (1967). Hollerbach and Flash (1982) demonstrated in simulation that the wrist paths resulting from ignored interaction torques at both joints of a two-jointed serial chain are not characteristic of human behavior. Subsequent studies showed that muscular control accounts for interaction effects (Abend et al. 1982; Galloway et al. 2004; Gribble and Ostry 1999; Karst and Hasan 1991a, b; Sainburg et al. 1995, 1999; Schneider et al. 1990; Virji-Babul and Cooke 1995).

The equilibrium-point approach of Feldman (1986) and the optimal-control approach of Todorov (2004) for studying motor control view the regulation of interaction effects as a by-product of their respective control strategies. In contrast, force control theories presume that interaction effects are represented in *internal models* (Kawato 1999)—neural constructs that mimic the input–output (or their inverse) relations of the motor apparatus—and are used to directly specify muscle forces (Hollerbach 1982). The leading joint hypothesis (LJH) (Dounskaia 2005; Dounskaia et al. 1998, 2002; Hirashima et al. 2007), which belongs to the last category, is an *inverse dynamical internal model*. It provides an algorithm for estimating the joint torques required to execute a desired hand trajectory. These torques are presumably converted into muscle activations by other internal models.

The governing equation for the inverse dynamics of a serial chain, ignoring dissipative forces at joints, may be expressed as (Murray et al. 1994)

$$\overline{T}_{muscle} = \mathbf{I}(\overline{q}) \cdot \ddot{\overline{q}} - \mathbf{C}(\overline{q}, \dot{\overline{q}}) - \overline{T}_{gravity}, \quad (1)$$

where $\overline{q}$ is the prescribed vector of joint displacements, **I** and **C** are the inertia and the Coriolis matrix, respectively, $\overline{T}_{gravity}$ is the vector of gravity-induced joint torques, and $\overline{T}_{muscle}$ is the vector of joint torques, presumably created by the activation of muscles spanning the joints, passive tendons, and the supporting skeletal structure. The dot notation indicates derivative with respect to time. The muscle torque expression for any single joint involves accelerations, velocities, and positions of all joints, since the matrices **I** and **C** are generally not diagonal. This is precisely the interaction effect, and in estimating the muscle torque at one joint, the central nervous system (CNS) must compensate for the torque induced by the motion of all other joints in the chain. Now, analysis of recorded human arm movements has revealed that the interaction effects at one joint are often low. The LJH suggests that the CNS ignores these low interaction effects while composing the task-specific torque at the *leading joint*, which serves as a dynamic foundation of the movement of the entire chain. Leading joint motion generates strong interaction torque at the other (*subordinate*) joints. The role of the subordinate-joint musculature is to regulate interaction torque and create net torque that results in the desired motion of the hand (Dounskaia 2005). This simplification in the movement dynamics leads to a corresponding simplification of joint-level control. Dounskaia (2005) also proposes a scheme decoupling the control of leading and subordinate joints into relatively independent hierarchical components.

The LJH gathers supporting evidence from a host of studies wherein joint torque analysis is used to determine the roles of leading and subordinate joints (Buchanann 2004; Dounskaia et al. 1998; Galloway and Koshland 2002; Hirashima et al. 2007; Ketcham 2004; Levin et al. 2001). Electromyographical (EMG) signals showing reciprocal bursts of activity at the leading joint that are tightly coupled with the joint's acceleration and deceleration (Dounskaia et al. 1998; Levin et al. 2001) offer further support. EMG activity at the subordinate joint is more complex. All of the studies cited above are planar motion studies, except Hirashima et al. (2007) in which the throwing motion of skilled baseball players is investigated. The objective of this paper is to extend the LJH to spatial reaching motion.

Methods

Subjects and tasks

Nine subjects, five female and four male, with no history of physical or neurological disorders participated in the study. Eight subjects were right handed, and one was ambidextrous. Subjects were between 20 and 33 years of age (mean = 23.22 years, standard deviation (SD) = 3.9 years) and naive to the purpose of the experiment. All subjects gave their informed consent prior to inclusion in the study. This research received approval from the appropriate Institutional Review Board.

The subjects sat in and were strapped to a chair with a band passing over the chest and under the arms to minimize the movement of the thorax. Eight colored tennis balls serving as targets were arranged around the subject on stands made of PVC pipe, as shown in Fig. 1. Table 1 specifies the locations of the targets relative to the subject's right shoulder (median values).

The following six reaching tasks, consisting of the subject pointing from an initial target to a final target with the right arm and depicted in Fig. 2, were used in the study.

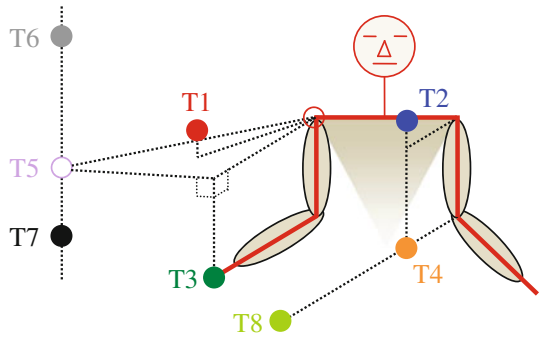

Fig. 1 Location of targets relative to subject's right shoulder. Tennis balls covered with colored paper serve as targets mounted on PVC pipe frames. *Dotted lines* indicate spatial locations of targets

Table 1 Target locations relative to right shoulder

Target	Distance from shoulder (m)	Azimuth (deg)	Elevation (deg)
T1	0.45	−20	10
T2	0.50	45	10
T3	0.55	0	−35
T4	0.65	45	−35
T5	0.90	−60	0
T6	1.40	−60	50
T7	1.0	−60	−30
T8	0.95	30	−25

Distances are accurate to 0.05 m and angles to 5°

Task 1: $T1 \rightarrow T8$, short contralateral movement, decreasing elevation.
Task 2: $T3 \rightarrow T6$, long ipsilateral movement, increasing elevation.
Task 3: $T1 \rightarrow T5$, short ipsilateral movement, horizontal.
Task 4: $T2 \rightarrow T7$, long contralateral movement, decreasing elevation.
Task 5: $T2 \rightarrow T6$, long contralateral movement, increasing elevation.

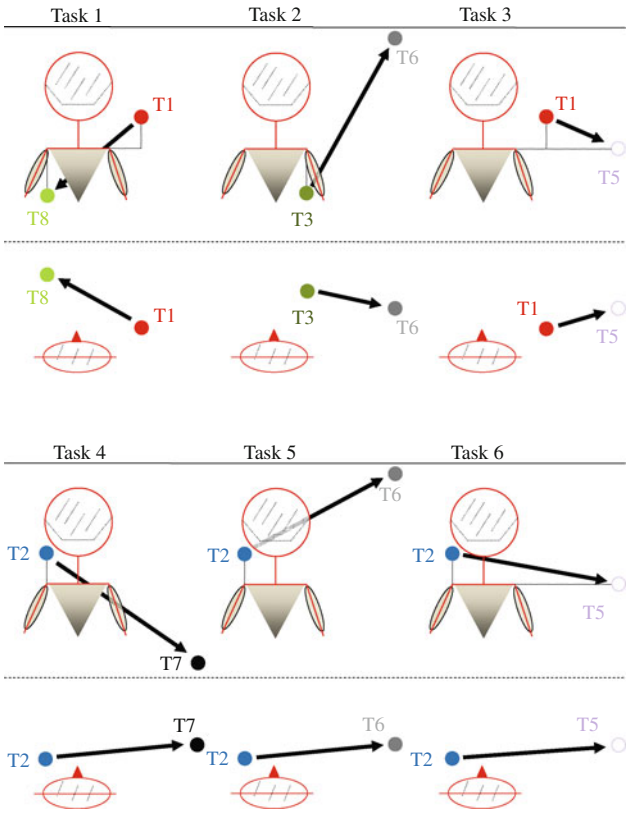

Fig. 2 Two views of each pointing task, one from behind subject and one overhead

Task 6: $T2 \rightarrow T5$, long contralateral movement, horizontal.

Two dummy tasks ($T4 \rightarrow T7$, and $T3 \rightarrow T7$) were included to provide enough tasks that subjects would not simply memorize joint motions for any one task. Subsequent analysis, however, indicated that these tasks were not necessary, so they are not considered further. All six tasks required movement away from the body and full extension of the elbow. Each began with the subject in the *neutral position* with the hands resting on the knees. The following instructions were given to the subject. *The experimenter will name the initial target. Point to the initial target with your forefinger close to the target and remain in that position. The experimenter will then call out a speed cue, followed by the final target. The speed cue will be either 'slow', 'normal', or 'fast'. Interpret the speed cue in a consistent fashion for various tasks. Move your head to locate the position of the final target (if necessary) and then point to the final target at the appropriate speed. Move the entire arm, i.e., the shoulder and the elbow, such that the elbow is maximally extended in the final position. Remain in the final position until the experimenter says the word 'neutral'. Return to the neutral position and wait for the specification of the next task. Keep the wrist rigid, and focus more on producing smooth movements rather than the accuracy of the final position of the finger.*[1]

Each subject performed 220 pointing motions. Of these, the first 20 involved all six tasks performed at all three speeds to acquaint the subject with the procedure. The actual experiment was comprised of the next 200 motions, including 20 repetitions of the dummy tasks, presented in pseudorandom order such that each task was repeated ten times at each of the three speeds. To minimize fatigue, breaks of approximately five minutes were enforced after the 80th, 130th, 170th, and 200th motions. None of the subjects reported feeling fatigued during the experiment.

Data recording and analysis

Electromagnetic sensors (Flock-of-Birds, Ascension Technology Corporation) were taped onto the subject's right wrist, right upper arm, right scapula, and spinous process of the 7th cervical vertebra. Sensor locations were related to various body-segment locations via a digitization protocol recommended by the International Society of Biomechanics (Wua et al. 2005). Local anatomical reference frames were defined for the right forearm, the right

[1] Movement at different speeds is not endemic to the discussion of the LJH. This feature of the experiment was included to evaluate the *Time Invariance Hypothesis* (Ambike and Schmiedeler 2006), which is not part of this paper.

upper arm, the right scapula, and the thorax, and joint reference frames were assigned to the shoulder and elbow joints. X, Y, and Z position coordinates were sampled at 100 Hz and filtered using a low-pass, fourth-order, zero-lag, Butterworth filter with a cut-off frequency of 1.5 Hz.

Kinematic model and movement kinematics

The arm is modeled as a three-link kinematic chain with idealized spherical and revolute joints at the shoulder and elbow, respectively. The wrist joint is ignored. The center of the glenohumeral joint is located using the rotation method (Veeger 2000), and it served as the center of the spherical joint of the kinematic model. The rotation axis of the elbow corresponds to one of the axes of the forearm's anatomical reference frame.

Movement kinematics, including up to third-order linear and angular motion properties of the upper arm and forearm, were computed in ***The MotionMonitor*** software (Innovative Sports Training, Inc.). These data were used to compute the kinematic quantities required for joint torque computation in the "Appendix". The detailed kinematic development is found elsewhere (Ambike 2011).

Movement dynamics

In previous LJH research (Dounskaia 2005; Dounskaia et al. 2002, 1998; Hirashima et al. 2007) and work involving serial chain, inter-segmental dynamics (Galloway and Koshland 2002; Hore et al. 2011; Sainburg et al. 1995, 1999; Sainburg and Kalakanis 2000; Schneider and Zernicke 1990), the torque components at a segment's proximal joint are partitioned into muscle torque (MT), interaction torque (IT), gravity torque (GT), and net torque (NT), related by

$$\overline{T}_{net} = \overline{T}_{muscle} + \overline{T}_{interaction} + \overline{T}_{gravity}. \quad (2)$$

Equation 2 is obtained from Equation 1 by partitioning the terms $\mathbf{I}(\overline{q}) \cdot \ddot{\overline{q}} - \mathbf{C}(\overline{q}, \dot{\overline{q}})$ using some rule based on the definitions of NT and IT to get $\overline{T}_{net}$ and $\overline{T}_{interaction}$.[2] Zatsiorsky (2002) provides an overview of the definitions of these torque components used in the literature. The contributions of MT and IT to NT at each joint for an entire movement are quantified from the time series of the torque components. This includes an analysis of torque signs, torque impulses, torque timing, and EMG recordings. Torque signs indicate the portion of the movement for which MT is dominant in accelerating the joint (Dounskaia et al. 1998; Sainburg et al. 1999). The signed impulses of the torque components indicate the magnitude of the contributions of MT and IT to NT (positive when in the same direction as NT). If the total IT impulse is small compared to the MT impulse, it is classified as ignorable. Relative timing of MT compared to NT is assessed as an absolute shift in time of MT-positive and MT-negative peaks relative to the corresponding NT peak in each cycle, divided by the cycle duration. This is close to zero if the peaks occur simultaneously, that is, when MT is the dominant component of NT. Deviation from zero indicates that IT contributes to NT, influencing its timing (Dounskaia et al. 2002). Finally, processed EMG signals from the anterior and posterior deltoids and from the biceps and lateral head of the tricep are compared with the NT profiles at the shoulder and elbow, respectively, to reveal the extent to which muscle activity directly caused joint acceleration/deceleration (Dounskaia 2005). Dounskaia et al. (1998) provide similar EMG analysis for arm movement involving the elbow and wrist joints.

A similar analysis is used in the present paper, but the equations of motion (EOM) for the spatial chain are written first. A set of definitions for the torque components are chosen and used to partition the EOM. The analysis of torque signs and impulses is modified to account for two characteristics unique to spatial motion—gravity and the non-collinearity of shoulder torque components. Analysis of torque timing is omitted since it reveals the same information as the analysis of torque impulses, and EMG measurements were not made. The objective is to determine whether IT at one joint is small compared to the corresponding MT so that it can be considered ignorable, as required by the LJH.

Euler's angular momentum balance equation (Greenwood 1988; Zatsiorsky 2002) applied to each segment of a serial chain (planar or spatial) is

$$\overline{M} = \mathbf{I} \cdot \overline{\alpha} + \overline{\omega} \times \mathbf{I} \cdot \overline{\omega}, \quad (3)$$

where $\overline{M}$ is the sum of all external moments acting on the segment, $\mathbf{I}$ is the segment's inertia tensor, and $\overline{\omega}$ and $\overline{\alpha}$ are the segment's angular velocity and angular acceleration, respectively. Equation 2 for a joint is obtained by partitioning the terms in Eq. 3 written for the limb segment distal to the joint. For planar chains, the second term in the right-hand side of Eq. 3, called the gyroscopic torque, vanishes, and $\overline{M}$ does not contain any term proportional to the square of the angular velocity of the limb segment. Consequently, the NT expression is proportional to the angular acceleration of the limb segment distal to the joint. Therefore, NT has been defined for planar motion as (Dounskaia 2005; Dounskaia et al. 2002; Zatsiorsky 2002)

[2] For a planar arm model, all joint torque vectors are normal to the arm's movement plane. Therefore, the torques in Eq. 2 appear as scalar magnitudes in the cited studies. In contrast, NT, MT, IT, and GT generally represent vector quantities in this paper, unless stated otherwise.

NT1: joint torque associated with the angular acceleration at the joint.

Elsewhere, NT is more generally defined as (Schneider and Zernicke 1990)

NT2: the sum of all the positive and negative torque components (gravitational, interactive, and muscle) that act at a joint.

For general 3D motion, terms proportional to the square of a segment's angular velocity arise from a non-trivial gyroscopic torque and the external moments, $\overline{M}$, in Eq. 3. Thus, *NT2* is the operative definition for net torque in this work. Additionally, this choice respects the previously used definition of IT (Galloway and Koshland 2002; Sainburg et al. 1999; Zatsiorsky 2002)

IT: torque component at a joint associated with acceleration and velocity at other joints.

This paper also adopts the previously used definitions of GT and MT (Schneider and Zernicke 1990):

GT: a passive torque resulting from gravity acting at the center of mass of each segment, and

MT: a 'generalized' torque that includes forces arising from active muscle contractions and from passive deformations of muscles, tendons, ligaments, and other periarticular tissues.

Using these definitions, Euler's equation for the forearm can be partitioned to obtain the elbow torque components. Any term containing *only* the elbow joint variable[3] and/or its derivatives is classified as NT. Any term that additionally contains the shoulder-joint variable and/or its derivatives is classified as IT. Any term containing the gravity vector is classified as gravity torque. These torque components are computed using the measured movement kinematics and anthropometric data (Dempster and Gaughran 1967) obtained from subject's weight and height, and MT is computed using Eq. 2. The same partitioning scheme is applied to Euler's equation for the upper arm, and shoulder torque components are obtained similarly.

Unlike horizontal-plane motion, a spatial arm motion study must contend with gravity-induced joint torques. Hollerbach and Flash (1982) proposed that the CNS may compute the gravity- and motion-dependent torques separately. The study found that gravity-independent NT profiles for performing reaching movements at different speeds were scaled by the square of the ratio of the movement times. This led to a motor control strategy wherein the motion-dependent torques for a given movement are obtained by scaling an existing record of torques required for the same motion, to which gravity torques are added separately. This argument has since been reiterated (Atkeson and Hollerbach 1985; Soechting 1986) and experimentally validated (Flanders and Herrmann 1992; Yadav 2010). Based on these arguments and experimental evidence, Eq. 2 is modified as follows.

$$\overline{T}^{*}_{muscle} := \overline{T}_{muscle} + \overline{T}_{gravity} = \overline{T}_{net} - \overline{T}_{interaction}.$$

Thus, the present paper removes gravity torques from the discussion of the LJH. The focus of the ensuing analysis is on quantifying the relations between $\overline{T}_{net}$, $\overline{T}_{interaction}$ and the portion of the muscle torque required to generate the motion torques, $\overline{T}^{*}_{muscle}$. In what follows, the * is dropped from $\overline{T}^{*}_{muscle}$, and the term 'muscle torque (MT)' as well as the notation $\overline{T}_{muscle}$ will refer to the gravity-separated muscle torque.

Adopting the single-degree-of-freedom (DOF) revolute-joint model for the elbow implies that the elbow torque components are collinear. Therefore, the elbow torque analysis is conducted without modification to the methods in Dounskaia (2005); Dounskaia et al. (1998, 2002). The torque about the elbow axis is provided by the elbow musculature, and the other component is provided passively by the surrounding skeletal structure. Therefore, scalar magnitudes are used for the elbow joint torque analysis, and NT, IT, and MT represent scalar torque magnitudes when referring to the elbow.

In contrast to the elbow, shoulder torque components are non-collinear, and MT, NT, and IT represent vector quantities. Here, MT (or IT) is called *assistive* when the angle between the NT and MT (or IT) vectors is less than 90° (the dot product is positive). When the angle is greater than 90°, MT (or IT) is called *resistive*. The analysis of signs now consists of computing the portion of the movement for which MT is assistive. For the torque impulse analysis, the impulses are computed by summing the component of MT (and IT) along NT over the duration of motion.

The component of MT normal to NT is called the *vestigial component*. It cancels the component of IT normal to NT and is quantified by computing the vestigial impulse factor, Ψ. At time i, the components of MT are related by the Pythagorean theorem,

$$|\overline{T}_{muscle-i}|^2 = |\overline{T}_{muscleP-i}|^2 + |\overline{T}_{muscleV-i}|^2,$$

where $\overline{T}_{muscleP-i}$ and $\overline{T}_{muscleV-i}$ are the components of $\overline{T}_{muscle-i}$ parallel and normal to NT, respectively. The vestigial impulse factor Ψ is

$$\Psi := \frac{\sum_i \overline{T}_{muscleV-i} \cdot \overline{T}_{muscleV-i}}{\sum_i \overline{T}_{muscle-i} \cdot \overline{T}_{muscle-i}}, \quad (4)$$

[3] The elbow joint variable is defined as the angle between the forearm and the upper arm.

and is bounded: $0 \leq \Psi \leq 1$. If the MT vector is mostly aligned with the NT vector, the component of MT normal to NT will be small, so $\Psi \rightarrow 0$. If the MT vector is almost normal to the NT vector, most of MT will counter IT, and $\Psi \rightarrow 1$.

Results

Classifying reaching movements

Characteristic results for one subject (JM) are provided in Figs. 3, 4, 5.

Tasks 1, 2, and 5

Figure 3 shows that MT was assistive at the shoulder for a longer duration than at the elbow. Furthermore, at the shoulder, MT was assistive for close to 100 % of the duration. Figure 4 shows that at the shoulder, the MT impulse was larger than the IT impulse. Conversely, the IT impulse at the elbow was almost equal to or greater than the MT impulse. Finally, Fig. 5 shows small values for Ψ. Thus, at the shoulder, most of MT was involved in generating NT. Conversely, MT and IT both contributed to generate NT at the elbow. Therefore, these movements are classified as a shoulder-led motion for all speeds.

Task 3

The shoulder and elbow exchange roles for this task. The analysis of torque signs shows that MT is assistive for a longer portion of the movement at the elbow than the shoulder. Elbow MT is assistive for close to 100 % of the duration, and the elbow MT impulse is greater than its IT impulse. The Ψ values suggest that the vestigial component of MT is small, but the shoulder IT impulse is much larger than its MT impulse. Therefore, the shoulder acts as a subordinate joint, and this motion is classified as elbow-led for all speeds.

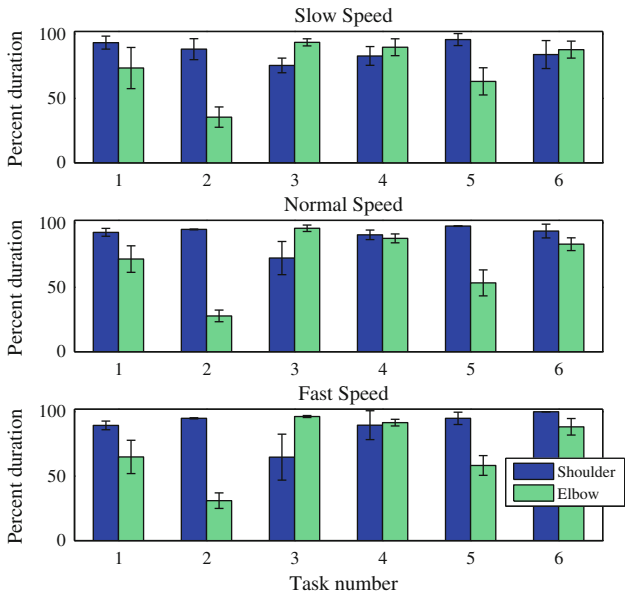

Fig. 3 Mean ± SD of duration of total movement for which MT is assistive. Subject JM

Task 4

In Fig. 3, MT is assistive at each joint for a similar, significant duration. For slow-speed movement, Fig. 4 shows low IT impulses at both joints, possibly due to low movement speed (peak wrist speed 0.7 ± 0.03 m/s for slow compared to 1.62 ± 0.01 m/s for fast movements). Furthermore, Ψ is low (0.2). Since interaction effects at both joints are low, it is proposed that both joints function independently and the control at each joint is decoupled. The normal-speed movement shows a low IT impulse at the elbow. The significant negative IT impulse at the shoulder is being suppressed by a high positive MT impulse, as corroborated by the low Ψ value of 0.15. Therefore, the normal-speed movement is classified as elbow-led. Significant negative IT impulses at both joints are being suppressed by high MT impulses for fast-speed movements. Therefore, this movement cannot be classified as shoulder- or elbow-led.

Task 6

Since all speeds of this task are similar to the normal- and fast-speed motions for Task 4, it is classified as elbow-led for all speeds.

Similar analysis was conducted for all nine subjects. The classification of all tasks for all subjects is provided in Table 2. Similar to prior planar studies, most motions are classified as shoulder-led, with relatively few classified as elbow-led. Additionally, very few movements (4 out of 162 and all in Tasks 4 and 6) are consistent with an 'independent-joint-control' strategy, while a few others (14 out of 162 and all in Tasks 1, 3, and 4) could not be classified in any of the three categories because large IT impulses were observed at both joints simultaneously.

Motions at two joints can be mechanically independent, as when joints move in orthogonal planes (Dounskaia 2005). A condition for almost mechanically independent joint motions is demonstrated here in the small interaction effects resulting from slow movement speeds. For serial chains with more than two joints, all joints with mechanically independent motions could be classified as leading joints (Dounskaia 2005). In the present case, since the

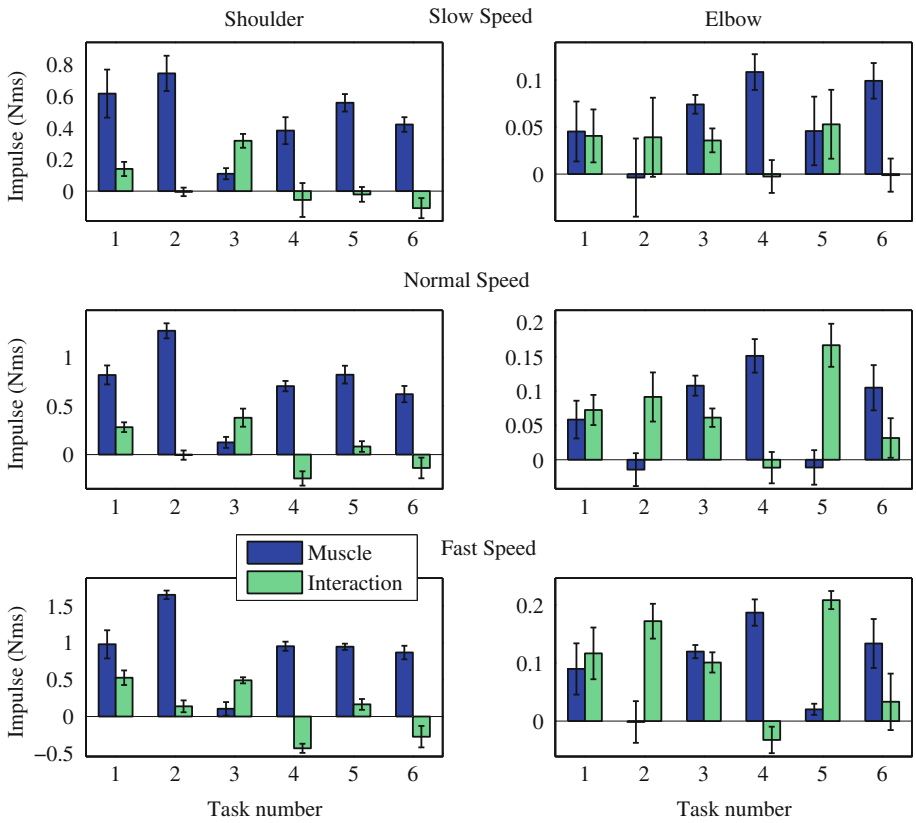

Fig. 4 Mean ± SD of MT and IT impulses at shoulder and elbow. Subject JM

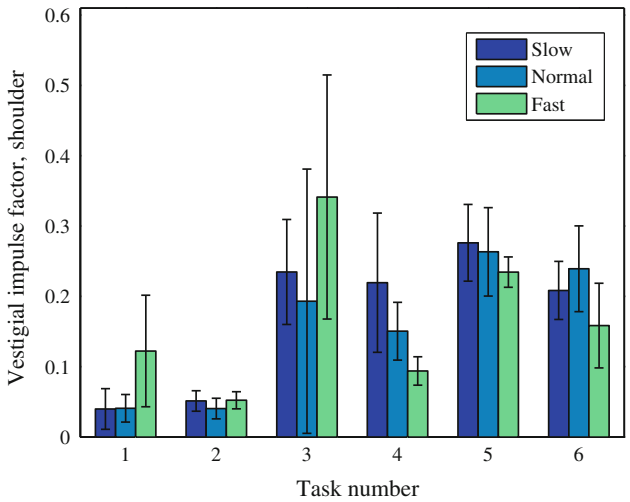

Fig. 5 Mean ± SD of the vestigial impulse factor Ψ at shoulder joint. Subject JM

chain has only two joints, mechanical independence of their motions makes independent joint control plausible.

Figure 6 shows the mean ± SD of the peak wrist speed and joint excursions for all tasks for subjects who exhibited the independent-joint-control strategy. The elbow excursion is the Euler-angle displacement along the *Z* axis of the anatomical frame attached to the upper arm. The *Z*-axis of the upper arm frame is oriented along the elbow joint rotation axis. The shoulder excursion is the angle obtained from the axis-angle parametrization (Spong 2006) relating the initial and final orientations of the upper arm coordinate frame for a movement. The joint excursions are averaged across all repetitions and speeds. For all three subjects, the slow-speed movement for Task 4 is classified as using independent joint control. For subject CR, the slow- and normal-speed movements for Task 6 are classified similarly. Figure 6 shows that the shoulder excursions for these movements are low. Thus, the low elbow IT impulse is the result of small shoulder velocity and acceleration.

Table 2 Classification of all movements

Subject	Task 1	Task 2	Task 3	Task 4	Task 5	Task 6
JM	SSS	SSS	EEE	IEN	SSS	EEE
AL	NNN	SSS	SSS	SSS	SSS	SSS
DE	SSS	SSS	NNN	ISS	SSS	SSS
FR	SSS	SSS	SSS	SSS	SSS	SSS
RR	SSS	SSS	EEN	SSS	SSS	EEE
CR	NNN	SSS	SSS	ISS	SSS	IIS
KB	NNN	SSS	SSS	EEE	SSS	SSS
JR	SSS	SSS	SSS	SSS	SSS	SSS
AS	SSS	SSS	SSS	SSS	SSS	SSS

S shoulder-led, *E* elbow-led, *I* independent joint control for all speeds ordered slow, medium, fast for each subject, *N* indicates that the motion could not be classified

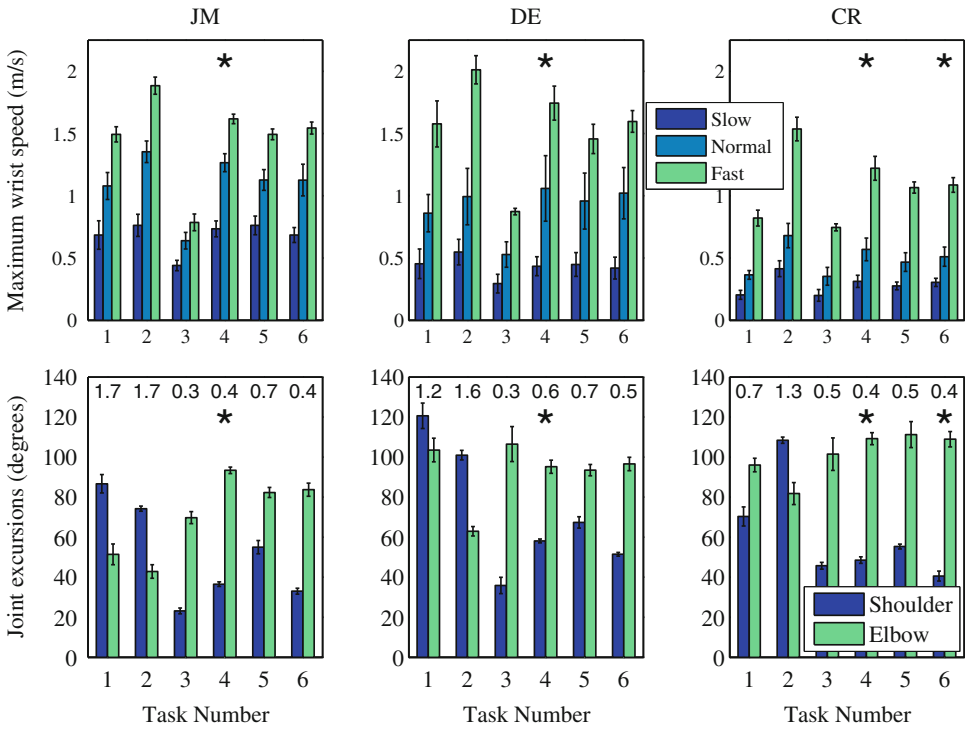

Fig. 6 Mean ± SD of peak wrist speeds and joint excursions for all tasks for subjects who exhibited independent-joint-control strategy in movements indicated by *asterisk*

Furthermore, some component of elbow IT will be orthogonal to the elbow joint axis, further reducing the IT impulse along the axis. Conversely, the elbow excursion is substantial for these motions, so the low shoulder IT impulse is attributed to the smaller inertia of the forearm. Still, the low shoulder IT impulse must also depend on the motion geometry. Compare subject CR's slow-speed movements of Tasks 3 and 4 for which the joint excursions are similar. Although Task 3 was performed more slowly than Task 4 (see Fig. 6), it is classified as shoulder-led, while Task 4 is classified as independent-joint-control motion. The geometry of the task must be influencing the shoulder IT.

Elbow-led movements and joint kinematics

A correlation between the leading joint and joint kinematics for cyclical tracing of shapes (Dounskaia 2005; Levin et al. 2001) as well as discrete arm movements (Galloway and Koshland 2002) has been identified in planar studies. Most movements are shoulder-led, with elbow-led motions typically observed when shoulder displacement is low and elbow displacement is high.

Figure 7 shows the mean joint excursions for the shoulder and elbow for all tasks for subjects who executed some elbow-led motions as marked by an asterisk. The number on top of each bar is the ratio of mean shoulder excursion to mean elbow excursion. Elbow-led motions typically have small excursion ratios ($\approx 0.3 - 0.4$) and small absolute shoulder excursions (<40°). However, some other motions with similar joint kinematics, such as Task 5 for subject RR and Task 6 for subject KB, are classified as shoulder-led. Additionally, subject DE (not shown in Fig. 7) shows similar joint kinematics with a mean shoulder excursion of 36° and an excursion ratio of 0.34 for Task 3, which is unclassifiable (see Table 2). Apart from three cases, the relation between the joint kinematics and leading joint observed for planar motion is strongly reproduced for spatial motion.

The results are summarized as follows.

Spatial arm movements are typically shoulder-led. Elbow-led movements occur when the shoulder excursion is low.

For some movements, low interaction effects are observed at both joints due to slow movement speed and motion geometry. In such cases, the joint motion is (almost) mechanically independent, so the CNS may employ an independent-joint-control strategy.

Discussion

An alternative to the torque-partitioning scheme presented here was developed by Hirashima et al. (2007). Their 'non-orthogonal torque decomposition' method decomposes a joint torque along three non-orthogonal, pose-dependent, effective axes. These axes are determined such

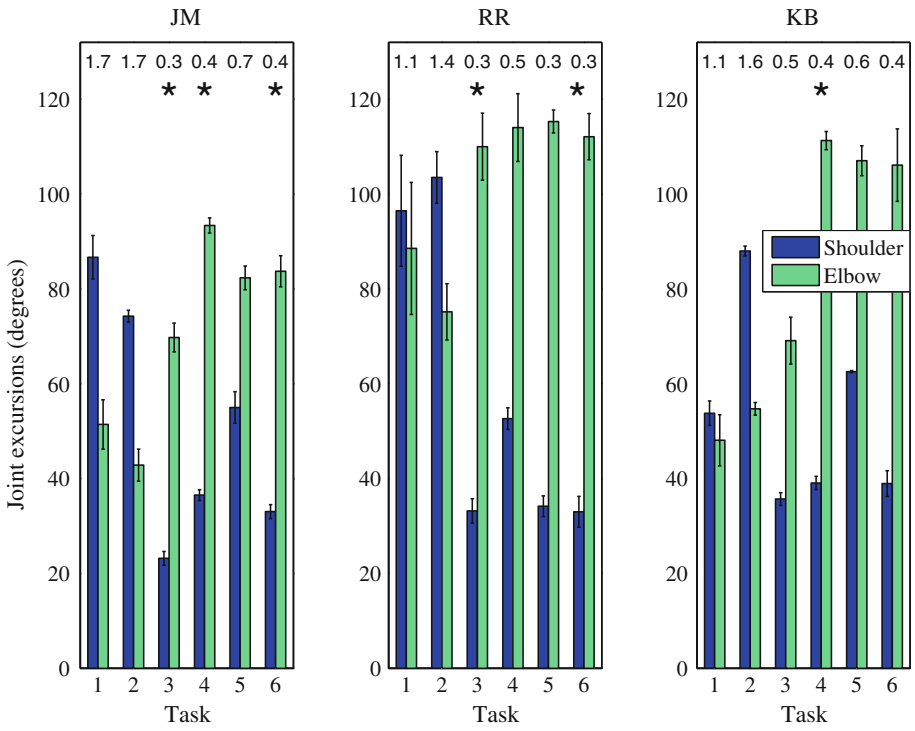

Fig. 7 Mean of joint excursions for subjects who exhibit elbow-led control strategies in movements indicated by *asterisk*. Number above each *bar* indicates excursion ratio

that a torque about each effective axis produces a joint rotation only about one of the joint coordinate axes. The method explains the cause–effect mechanism whereby three angular accelerations at the shoulder, for example, are produced by the resultant joint torque, gravity torque, and IT. The approach is particularly useful to reveal the mechanical cause of a joint rotation about each joint coordinate axis of a multi-DOF joint. However, the segment angular velocity-dependent gyroscopic terms in Euler's equation are classified as IT, which is, therefore, no longer torque resulting solely from motion at other joints.

Dounskaia (2005) proposed an elegant, hybrid control scheme that exploits the simplified dynamics of the LJH for planar arm motion. This scheme simplifies shoulder-joint control for shoulder-led motions. The required shoulder torque for a movement is obtained using a lookup table organized as a simple association between a gross description of the required movement—for example, initial and final joint position, movement time, and expected inertial resistance of the limb—and torque. This control strategy for the (proximal) leading joint replaces complex inverse kinematics and dynamic computations with simpler memory recalls. The control at the subordinate joint employs structured algorithms that compute MT from joint kinematics using constant inertial parameters. These algorithms account for the interaction effects created by the leading joint motion and produce task-specific arm motions.

Equations 5 and 8 show that NT for spatial motion is a linear function of the joint angular acceleration and a nonlinear function of the joint angular velocity. The latter complicates shoulder-joint control for spatial motion, but the hybrid control algorithm of Dounskaia (2005) still applies. The shoulder torque for a movement may yet be obtained via a lookup table using an association between a comparatively more complex gross description of the required movement and torque. The motion characteristics used to construct this mapping will be similar to those in the planar case. Note that ignoring the interaction terms (Eqs. 6, 9) in the leading joint torque expression is a significant simplification of the EOM for the leading joint. There is no change in the strategy for the subordinate-joint control. Thus, the LJH and the associated control scheme are both plausible explanations for spatial arm motion control.

While low interaction effects at the most proximal joint in a serial multi-joint chain appear to be a general phenomenon, exceptions do exist. Leading and subordinate joints switch roles for movements that require low proximal-joint excursion and high distal-joint excursion. Also, low interaction effects at *both* joints appear for slow movements and movements with decoupled joint motions (Dounskaia 2005). Now, control of the proximal joint in a serial chain is the more complex problem, and simplification of overall control is achieved by simplifying the dynamics of that joint. So, for elbow-led movements, the advantage of simplified dynamics does not seem to transfer

to joint control for movements that require muscular regulation of the shoulder-joint IT. Conversely, for movements with mechanically independent joint motions, the joint-level control is presumably simpler than that for shoulder-led movements.

Certain arm movements are unlikely to be observed in natural human behavior. The experimental protocol may have elicited some such behavior in the present study. Arm geometry dictates that wrist-movement directions that require muscular suppression of subordinate-joint IT are less common than directions in which the subordinate-joint IT assists the generation of the desired wrist movement (Dounskaia 2005). Furthermore, Goble et al. (2007) show that movements requiring muscular regulation of the subordinate-joint interaction effects are less preferred compared to movements wherein the subordinate joint moves passively in the influence of IT. Both results were demonstrated for planar movement, but they likely extend to unconstrained spatial movements as well. Some unclassifiable movements (Task 3 for subject DE and the fast-speed movement for Task 4 for subject JM) may be unpreferred movements as described by Goble et al. (2007), because MT and IT impulses are simultaneously large at both joints. Some elbow-led movements (Task 6 for subjects JM and RR, and Task 4 for subject KB) show significant shoulder-joint MT and, therefore, may also be unpreferred movements.

The muscle torques $\overline{T}^{*}_{muscle}$ used in the analysis represent the muscular effort required to produce motion. To these 'motion torques' are added torque estimates that compensate for gravity, so the final torque command consists of a motion-dependent component plus a position-dependent gravity component, likely produced by different neural mechanisms. Thus, the spatial extension of the LJH herein proposes a method for estimating the gravity-separated component of muscle torques. For a reaching motion in which the arm-segment elevation decreases, the muscle torque would likely be reduced in magnitude early in the movement (only needed when the speed of movement is greater than what gravity would produce on its own) and likely opposite in sign near the end of the movement to hold the arm up against gravity. In such cases, the control strategy may be to allow gravity torques to dominate and to simply modulate muscle torques to yield the desired motion, again perhaps largely ignoring interaction effects, at least at one joint. Also, for preferred movements (Goble et al. 2007), the subordinate joint may move passively under the influence of interaction and gravity effects. Comparing the gravity impulse with the impulse of $\overline{T}_{muscle}$ due to total muscular effort might help to identify such movements and determine whether the joints were 'gravity driven' or 'muscle driven'.

For planar arm motion, NT at both joints is proportional to the joint acceleration. Pronounced reciprocal bursts of activity in the EMG profiles of anterior and posterior deltoids whose timing is tightly coupled with the timing of peak shoulder acceleration and deceleration are presented as validating evidence for the LJH (Dounskaia 2005; Dounskaia et al. 2002; Levin et al. 2001). In contrast, Vandenberghe et al. (2010) recently observed EMG activity of the elbow and shoulder muscles during spatial reaching movement that was significantly different from the burst pattern reported during planar studies. Muscle activity was affected by target location and gravity, and activity of the shoulder muscles was found to increase before elbow muscles, inducing shoulder elevation prior to elbow extension. The role of the shoulder as the movement initiator for spatial reaching movements was validated.

Note that MT does not depend on the definitions of NT and IT. However, the analysis of joint control depends on NT and IT. Furthermore, the definitions of NT and IT adopted in this study attribute a definite, consistent role to the shoulder musculature in motion production. In Eq. 8, inertial and position characteristics of the forearm are included in the expression for shoulder-joint NT. This implies that the shoulder musculature controls this single, three-DOF, spherical joint, considering the inertia of the entire arm rather than just the upper arm.

Conclusions

A set of consistent definitions for the net torque and the interaction torque for spatial, multi-joint mechanisms was selected from the literature, and a torque impulse analysis for spatial movement was developed. Most movements in this study were classified as shoulder-led movements. A small number, typically associated with small shoulder excursions and large elbow excursions, were classified as elbow-led. Additionally, a few movements showed small interaction torque impulse at both joints due to slow movement speed and motion geometry. Such joint motion is mechanically independent, and the CNS may employ an independent-joint-control strategy in these cases. The LJH is a valid inverse dynamics algorithm for spatial arm reaching. The advantages of simplified movement dynamics were shown to transfer to simplified joint-level control. The scheme outlined by Dounskaia (2005) is, therefore, a potential control algorithm for spatial arm movement.

Acknowledgments Support was provided by grant no. IIS-0937612 from the National Science Foundation. The authors wish to thank Mr. Julian Corona for his assistance with the data collection.

Appendix

The analytical expressions for the net, interaction, and muscle torques for the shoulder and elbow joints developed in Ambike (2011) are provided here. The thorax is assumed to be stationary. The elbow is modeled as a single-DOF revolute joint with the rotation axis along the Z axis of the coordinate frame fixed in the upper arm, as recommended by the ISB protocol (Wua et al. 2005). The shoulder is modeled as a ball-and-socket joint allowing three degrees of rotational freedom for the humerus. The glenohumeral center was assumed as the joint center. The wrist joint is ignored. The hand is incorporated as a point mass at the end of the forearm, as seen in Fig. 8. The mass and center of mass of the combined 'forearm-hand' are computed and used in the torque calculations. In Ambike (2011), the development in Feltner and Dapena (1989), Gagnon and Gagnon (1992), Winter (2005) is modified by introducing movement of the forearm relative to the upper arm.

Figure 8 shows the global coordinate frame, frames attached to the forearm (F) and upper arm (U), and the free body diagrams of the arm segments. All variables are defined in Table 3. For a vector quantity, the leading superscript indicates the coordinate frame in which the vector is expressed, but the superscript is omitted for the global frame. The Newton–Euler approach (Winter 2005) for developing the equations of motions is more suitable

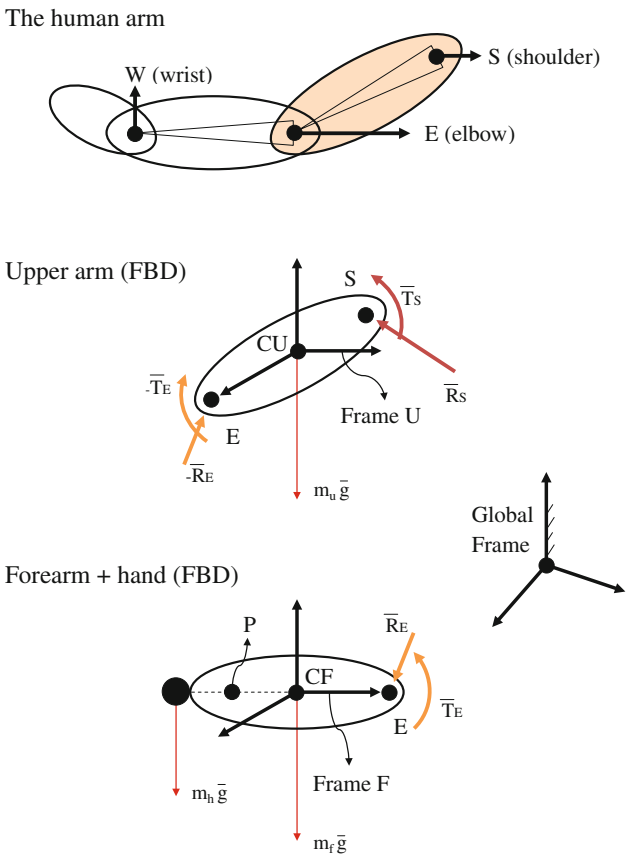

Fig. 8 Free body diagrams of upper arm and forearm. Hand is modeled as point mass rigidly attached to forearm

Table 3 Symbols for the reaction forces and joint torque expressions

Symbol	Description
${}^{A}\mathbf{R}_{B}$	Rotation matrix expressing the orientation of frame B in frame A
m_f	Mass of forearm
m_u	Mass of upper arm
M_{fh}	Combined mass of forearm and hand
I_U	Inertia matrix of upper arm
I_F	Inertia matrix of forearm
${}^{*}\overline{\omega}_u$	Absolute angular velocity of upper arm expressed in frame '*'
${}^{*}\overline{\alpha}_u$	Absolute angular acceleration of upper arm expressed in frame '*'
${}^{*}\overline{\omega}_{fu}$	Angular velocity of the forearm relative to the upper arm measured in frame U and expressed in frame '*'
${}^{*}\overline{\alpha}_{fu}$	Angular acceleration of the forearm relative to the upper arm measured in frame U and expressed in frame '*'
P	Center of gravity of the forearm and hand
$\overline{a}_{pf}$	Contribution of forearm movement in linear acceleration of P
$\overline{a}_{pu}$	Contribution of upper arm movement in linear acceleration of P
$\overline{a}_{pint}$	Interaction term in linear acceleration of P
$\overline{a}_u$	Linear acceleration of CU
${}^{A}\overline{r}_{B/C}$	Position vector from point C to point B expressed in frame A

than the Lagrangian approach (Greenwood 1988) for implementing the partitioning scheme outlined in "Data recording and analysis". Newton's second law applied to each segment yields the joint reaction forces, $\overline{R}_E$ and $\overline{R}_F$, at the elbow and the shoulder, respectively. The partitioning scheme is first applied to the reaction forces to obtain reaction components that can be attributed to motions of only the elbow ($\overline{R}_{EF}, \overline{R}_{SF}$), only the shoulder ($\overline{R}_{EU}, \overline{R}_{SU}$), both joints ($\overline{R}_{Eint}, \overline{R}_{Sint}$), and gravity ($\overline{R}_{Eg}, \overline{R}_{Sg}$).

$$\overline{R}_E = \overline{R}_{EF} + \overline{R}_{EU} + \overline{R}_{Eint} + \overline{R}_{Eg},$$

where

$$\overline{R}_{EF} = M_{fh}\overline{a}_{pf}, \quad \overline{R}_{EU} = M_{fh}\overline{a}_{pu},$$
$$\overline{R}_{Eint} = M_{fh}\overline{a}_{pint}, \quad \overline{R}_{Eg} = -M_{fh}\overline{g}.$$

Similarly, for the shoulder joint,

$$\overline{R}_S = \overline{R}_{SU} + \overline{R}_{SF} + \overline{R}_{Sint} + \overline{R}_{Sg},$$

where

$$\overline{R}_{SU} = m_u\overline{a}_u + \overline{R}_{EU}, \quad \overline{R}_{SF} = \overline{R}_{EF},$$
$$\overline{R}_{Sint} = \overline{R}_{Eint}, \quad \overline{R}_{Sg} = -(M_{fh} + m_u)\overline{g}.$$

Two applications of Euler's equation yield the net, interaction, and gravity torques at the elbow,

$$\begin{aligned} {}^F\overline{T}_{Enet} = & I_F \cdot {}^F\overline{\alpha}_{fu} + {}^F\overline{\omega}_{fu} \times I_F \cdot {}^F\overline{\omega}_{fu} \\ & - {}^F\overline{r}_{E/CF} \times {}^F\overline{R}_{EF}, \end{aligned} \tag{5}$$

$$\begin{aligned} {}^F\overline{T}_{Eint} = & I_F \cdot ({}^F\overline{\alpha}_u + {}^F\overline{\omega}_u \times {}^F\overline{\omega}_{fu}) \\ & + {}^F\overline{\omega}_{fu} \times I_F \cdot {}^F\overline{\omega}_u \\ & + {}^F\overline{\omega}_u \times I_F \cdot ({}^F\overline{\omega}_u + {}^F\overline{\omega}_{fu}) \\ & - {}^F\overline{r}_{E/CF} \times ({}^F\overline{R}_{EU} + {}^F\overline{R}_{Eint}), \end{aligned} \tag{6}$$

$${}^F\overline{T}_{Eg} = -{}^F\overline{r}_{E/CF} \times {}^F\overline{R}_{Eg} - {}^F\overline{r}_{W/CF} \times m_h^F\overline{g}, \tag{7}$$

and at the shoulder,

$$\begin{aligned} {}^U\overline{T}_{Snet} = & I_U \cdot {}^U\overline{\alpha}_u + {}^U\overline{\omega}_u \times I_U \cdot {}^U\overline{\omega}_u \\ & - {}^U\overline{r}_{S/CU} \times {}^U\overline{R}_{SU} + {}^U\overline{r}_{E/CU} \times {}^U\overline{R}_{EU} \\ & + {}^U\mathbf{R}_F\big(I_F \cdot {}^F\overline{\alpha}_u + {}^F\overline{\omega}_u \times I_F \cdot {}^F\overline{\omega}_u \\ & - {}^F\overline{r}_{E/CF} \times {}^F\overline{R}_{EU}\big), \end{aligned} \tag{8}$$

$$\begin{aligned} {}^U\overline{T}_{Sint} = & {}^U\mathbf{R}_F\big({}^F\overline{T}_{Enet} + I_F \cdot ({}^F\overline{\omega}_u \times {}^F\overline{\omega}_{fu}) \\ & + {}^F\overline{\omega}_u \times I_F \cdot {}^F\overline{\omega}_{fu} + {}^F\overline{\omega}_{fu} \times I_F \cdot {}^F\overline{\omega}_u \\ & - {}^F\overline{r}_{E/CF} \times {}^F\overline{R}_{Eint}\big) \\ & - {}^U\overline{r}_{S/CU} \times ({}^U\overline{R}_{SF} + {}^U\overline{R}_{Sint}) \\ & + {}^U\overline{r}_{E/CU} \times ({}^U\overline{R}_{EF} + {}^U\overline{R}_{Eint}), \end{aligned} \tag{9}$$

$${}^U\overline{T}_{Sg} = -{}^U\mathbf{R}_F\,{}^F\overline{T}_{Eg} - {}^U\overline{r}_{S/CU} \times {}^U\overline{R}_{Sg}. \tag{10}$$

References

Abend W, Bizzi E, Morasso P (1982) Human arm trajectory formation. Brain 105:331–348

Ambike S, Schmiedeler JP (2006) Modeling time invariance in human arm-motion coordination. In: Lenarčič J, Roth B (eds) Advances in robot kinematics. Springer, Dodrecht, pp 177–184

Ambike SS (2011) Characteristics of spatial human arm motion and the kinematic trajectory tracking of similar serial chains. Dissertation, The Ohio State University

Atkeson CG, Hollerbach JM (1985) Kinematic features of unrestrained vertical arm movements. J Neurosci 5:2318–2330

Bernstein NA (1967) The coordination and regulation of movement. Pergamon, New York

Buchanann JJ (2004) Learning a single limb multijoint coordination pattern: the impact of a mechanical constraint on the coordination dynamics of learning and transfer. Exp Brain Res 156:39–54

Dempster WT, Gaughran GRL (1967) Properties of body segments based on size and weight. Am J Anat 120:33–54

Dounskaia N (2005) The internal model and the leading joint hypothesis: implications for control of multi-joint movements. Exp Brain Res 166:1–16

Dounskaia N, Ketcham CJ, Stelmach GE (2002) Commonalities and differences in control of various drawing movements. Exp Brain Res 146:12–25

Dounskaia NV, Swinnen SP, Walter CB, Spaepen AJ, Verschueren SMP (1998) Hierarchical control of different elbow-wrist coordination patterns. Exp Brain Res 121:239–254

Feldman AG (1986) Once more for the equilibrium point hypothesis (λ model). J Mot Behav 18:17–54

Feltner ME, Dapena J (1989) Three-dimensional interactions in a two-segment kinematic chain. Part 1:general model. Int J Sports Biomech 5:403–419

Flanders M, Herrmann U (1992) Two components of muscle activation: scaling with the speed of arm movement. J Neurophysiol 67:931–943

Gagnon D, Gagnon M (1992) The influence of dynamic factors on triaxial net muscular moments at the L5/Sl joint during asymmetrical lifting and lowering. J Biomech 25:891–901

Galloway JC, Koshland GF (2002) General coordination of shoulder, elbow and wrist dynamics during multijoint arm movements. Exp Brain Res 142:163–180

Galloway JC, Bhat A, Heathcock JC, Manal K (2004) Shoulder and elbow joint power differ as a general feature of vertical arm movements. Exp Brain Res 157:391–396

Goble JA, Zhang Y, Shimansky Y, Sharma S, Dounskaia NV (2007) Directional biases reveal utilization of arm's biomechanical properties for optimization of motor behavior. J Neurophysiol 98:1240–1252

Greenwood DT (1988) Principles of dynamics. Prentice Hall, New Jersey

Gribble PL, Ostry DJ (1999) Compensation for interaction torques during single and multijoint limb movement. J Neurophysiol 82:2310–2326

Hirashima M, Kudo K, Ohtsuki T (2007) A new non-orthogonal decomposition method to determine effective torques for three-dimensional joint rotation. J Biomech 40:871–882

Hirashima M, Kudo K, Watarai K, Ohtsuki T (2007) Control of 3D limb dynamics in unconstrained overarm throws of different speeds performed by skilled baseball players. J Neurophysiol 97:680–691

Hollerbach JM (1982) Computers, brains, and the control of movement. Trends Neurosci 6:189–192

Hollerbach JM, Flash T (1982) Dynamic interactions between limb segments during planar arm movement. Biol Cybern 44:67–77

Hore J, Debicki DB, Gribble PL, Watts S (2011) Deliberate utilization of interaction torques brakes elbow extension in a fast throwing motion. Exp Brain Res 211:63–72

Karst GM, Hasan Z (1991a) Initiation rules for planar, two-joint arm movements: agonist selection for movements throughout the work space. J Neurophysiol 66:1579–1593

Karst GM, Hasan Z (1991b) Timing and magnitude of electromyographic activity for two-joint arm movements in different directions. J Neurophysiol 66:1579–1593

Kawato M (1999) Internal models for motor control and trajectory planning. Curr Opin Neurobiol 9:718–727

Ketcham CJ, Dounskaia N, Stelmach GE (2004) Age-related differences in the control of multijoint movements. Motor Control 8:422–436

Levin O, Ouamer M, Steyvers M, Swinnen SP (2001) Directional tuning effects during cyclical two-joint arm movements in the horizontal plane. Exp Brain Res 141:471–484

Murray RM, Li Z, Sastry SS (1994) A mathematical introduction to robotic manipulation. CRC Press LLC, Florida

Sainburg RL, Ghez C, Kalakanis D (1999) Intersegmental dynamics are controlled sequential anticipatory, error correction, and postural mechanisms. J Neurophysiol 81:1045–1056

Sainburg RL, Ghilardi MF, Poizner H, Ghez C (1995) Control of limb dynamics in normal subjects and patients without proprioception. J Neurophysiol 73:820–835

Sainburg RL, Kalakanis D (2000) Differences in control of limb dynamics during dominant and nondominant arm reaching. J Neurophysiol 83:2661–2675

Schneider K, Zernicke RF (1990) A FORTRAN package for the planar analysis of limb intersegmental dynamics from spatial coordinate-time data. Adv Eng Softw 12:123–128

Schneider K, Zernicke RF, Ulrich BD, Jensen JL, Thelen E (1990) Understanding movement control in infants through the analysis of limb intersegmental dynamics. J Mot Behav 25:521–535

Soechting JF, Lacquaniti F, Terzuolo CA (1986) Coordination of arm movements in three-dimensional space. Sensorimotor mapping during drawing movement. Neuroscience 17:295–311

Spong WM, Hutchinson S, Vidyasagar M (2006) Robot modeling and control. Wiley, USA

Todorov E (2004) Optimality principles in sensorimotor control. Nat Neurosci 7:907–915

Vandenberghe A, Levin O, De Schutter J, Swinnen S, Jonkers I (2010) Three-dimensional reaching tasks: effect of reaching height and width on upper limb kinematics and muscle activity. Gait Posture. 32:500–507

Veeger HEJ (2000) The position of the rotation center of the glenohumeral joint. J Biomech 33:1711–1715

Virji-Babul N, Cooke JD (1995) Influence of joint interactional effects on the coordination of planar two-joint arm movements. Exp Brain Res 103:451–459

Winter DA (2005) Biomechanics and motor control of human movement. Wiley, New Jersey

Wua G, van der Helm FCT, Veeger HEJ, Makhsouse M et al (2005) ISB recommendation on definitions of joint coordinate systems of various joints for the reporting of human joint motion. Part II: shoulder, elbow, wrist and hand. J Biomech 38:981–992

Yadav V (2010) Validation of a time-scaling-based model for representation of dynamics in humans and its applications in rehabilitation. Dissertation, The Ohio State University

Zajac FE, Gordon ME (1989) Determining muscle force and action in multiarticular movement. Exerc Sports Sci Rev 17:187–230

Zatsiorsky VM (2002) Kinetics of human motion. Human Kinetics, Champaign